

Nonrelativistic two-photon electron bremsstrahlung in a Coulomb field, including retardation

M. Dondera and Viorica Florescu

Faculty of Physics, University of Bucharest, P. O. Box 5211, Bucharest-Magurele, 76900 Romania

(Received 14 October 1997)

We study retardation effects in the two-photon electron bremsstrahlung in a Coulomb field, for the electron energy range 1–10 keV. The calculation is based on an exact analytic expression for the matrix element of the process, in a nonrelativistic treatment including retardation. The comparison with previous results for the Coulomb case (exact Coulomb dipole approximation or Born approximation with retardation) confirms the importance of retardation effects in the electron energy range under investigation, as indicated before by the Born approximation. [S1050-2947(98)02009-5]

PACS number(s): 34.80.-i, 32.80.Wr

I. INTRODUCTION

The simultaneous emission of two photons in an electron-atom collision, called two-photon or double bremsstrahlung, has received some attention several years ago, stimulated by the experimental observation of Altman and Quarles [1] of two photons in coincidence in electron-thin-solid-target interaction. Other experiments have been performed since, by Quarles and co-workers (see [2] for the most recent account) and by Hippler [3,4]. The electron energy range was different for the two sets of experiments: around 70 keV in Quarles's case, and around 10 keV in Hippler's case. Particular configurations have been recorded, namely, incident electron momentum along the bisectrice of the angle 2θ between the two emitted photons (denoted as the $\pm\theta$ geometry) for $\theta=45^\circ$ and $\theta=90^\circ$.

On the theoretical side the situation was briefly revised in [5]. The majority of the calculations reported up to now refer to the case of the electron scattering taking place in the Coulomb field of a fixed nucleus of charge Z [6–9]. An interesting approach has been developed by Korol [10], exploiting the properties of the momentum operator matrix element between two continuum states.

The orders of magnitude disagreement between the experimental data in the $\pm 45^\circ$ geometry and the Coulomb field results obtained in nonrelativistic dipole approximation (see Fig. 2 of Ref. [11]) at electron energies of 70 keV was an indication of the inadequacy of the dipole approximation. In the same conditions a relativistic Born approximation derived by Smirnov [12] was in reasonable agreement with the experiment [13–15]. The importance of retardation effects was confirmed afterwards in two different calculations [16,17]. In our previous paper [16], we have adopted a nonrelativistic Born approximation including retardation treatment, in an exploratory study of retardation effects. We have found that retardation effects are important even for energies in the 1–10 keV range. In a recent calculation [17], Korol has used the approximate method developed in [10] for the evaluation of the nonrelativistic matrix element of the double bremsstrahlung with retardation included. The numerical evaluations of the cross section in [17] bring more evidence on the importance of retardation effects, and are in agreement with [16]. Korol's approach seems to include in a satisfactory way the Coulomb effects.

Before the completion of our numerical calculation presented here, Korol [18] published analytical and numerical results on the two-photon bremsstrahlung, taking into account retardation. It appears that we have used the same analytic method, but due to different algebraic manipulations, we have obtained more compact expressions for several invariant amplitudes. For this reason, in this paper (i) we shall present our analytic results, but we shall omit details on their derivation, which employs the technique used in the dipole approximation by Véniard and co-workers [7], as Korol also does; (ii) we shall focus on the numerical predictions, in the energy range 1–10 keV for the incident electron, where the neglect of relativistic effect is justified, which is not always the case for energies around 70 keV, considered by Korol.

The matrix element of two-photon bremsstrahlung, in an exact nonrelativistic treatment, including retardation, is presented in Sec. II. Our results for the invariant amplitudes are given in the Appendix, with the exception of one of the amplitudes, discussed in more detail in Sec. II. This amplitude requires a special treatment, in connection with the δ -type behavior of the matrix element in the free electron case. Section III of this paper contains numerical results for two types of cross sections: σ_4 , which corresponds to the detection of the emitted photons only [see Eq. (13) here] and σ_5 , which describes the electron angular distribution at fixed photon geometry. The discussion starts with a comparison with experimental data obtained by Hippler for σ_4 , displayed in Fig. 1, corresponding to $\pm 90^\circ$ geometry. As explained previously [16], this geometry is least affected by retardation effects. Because there are no other experimental data in the incident electron energy range we investigate, the theoretical results presented in the other figures are selected in order to illustrate the importance of the retardation effects and some of their features, with the hope that new experimental data will be available.

We use the same notations as in [16] in order to designate the different approaches used in the Coulomb case: (i) BNRR—nonrelativistic Born approximation, with retardation included; (ii) CNRD—nonrelativistic dipole approximation, treating exactly the electron in a Coulomb field; (iii) CNRR—nonrelativistic “exact” calculation, retardation included. The cases presented in Sec. III and other cases we have considered show that (i) the validity of BNRR calcula-

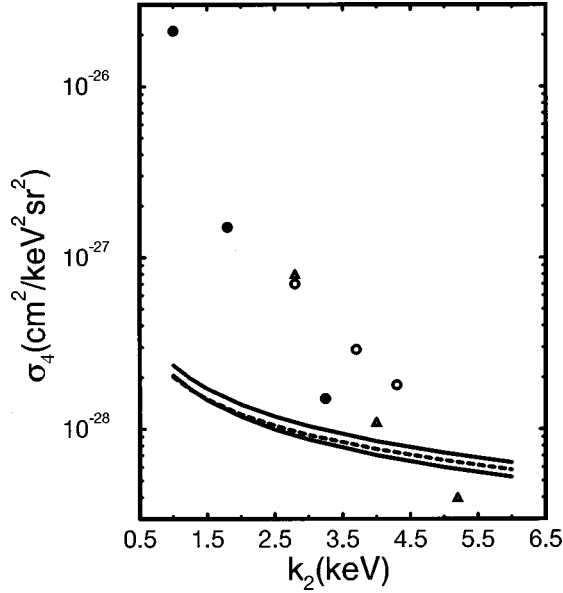


FIG. 1. The cross section σ_4 in the CNRR calculations, as a function of the photon energy k_2 , for $Z=54$ and the geometry $\pm 90^\circ$. For comparison, Hippler's experimental points are shown (without error bars). The results correspond to $T_1=8.82$ keV, $k_1=2.8$ keV for dashed curve and solid circles, $T_1=10$ keV, $k_1=2$ keV, for upper curve and open circles, $T_1=12.5$ keV, $k_1=2$ keV, for lower full curve and open triangles.

tion (equations presented in [16]) is restricted to high energies (usually tens of keV), but not too high because the relativistic effects begin to play a significant role, and low atomic numbers; (ii) the validity of CNRD (see [6,8]) is generally limited to low electron energies excepting the case of a special emission geometry (the two photons emitted orthogonal on the incident electron direction), for which the retardation effects are very small. Our study clearly indicates the need to use the CNRR calculation, to cover the range of electron energies between 1 keV and 20 keV, where the two approximations are in difficulty.

II. THE MATRIX ELEMENT

We denote the asymptotic electron momenta by \vec{p}_1 and \vec{p}_2 , the photon momenta by \vec{K}_1 and \vec{K}_2 , with photon direc-

tions specified by the unit vectors \vec{n}_1 and \vec{n}_2 , and the photon polarization vectors by \vec{s}_1 and \vec{s}_2 . The corresponding energies T_1, T_2, k_1 , and k_2 are connected by the conservation law $T_1=T_2+k_1+k_2$, and the momentum transfer is $\vec{\Delta}=\vec{p}_1-\vec{p}_2-\vec{K}$, with $\vec{K}=\vec{K}_1+\vec{K}_2$.

The amplitude \mathcal{M} of the two-photon bremsstrahlung is given by the Kramers-Heisenberg-Waller matrix element between initial and final continuum energy eigenstates $|\vec{p}_1+\rangle$ and $|\vec{p}_2-\rangle$. The asymptotic behavior at large distance is that of a distorted plane wave plus an outgoing or incoming wave for $\langle \vec{r}|\vec{p}_1+\rangle$ or $\langle \vec{r}|\vec{p}_2-\rangle$, respectively. The amplitude \mathcal{M} can be written as

$$\mathcal{M} = \sum_{i,j=1}^3 [\Pi_{ij}(\vec{K}_1, \vec{K}_2, \Omega_1) + \Pi_{ji}(\vec{K}_2, \vec{K}_1, \Omega_2)] s_1^* s_2^* + \mathcal{O} s_1^* \cdot s_2^*, \quad (1)$$

where we have denoted

$$\begin{aligned} \Pi_{ij}(\vec{K}_1, \vec{K}_2, \Omega) &= \frac{1}{m_e} \left\langle \vec{p}_2- \left| \exp\left(-\frac{i}{\hbar} \vec{K}_2 \cdot \vec{R}\right) P_j G(\Omega) P_i \right. \right. \\ &\quad \left. \left. \times \exp\left(-\frac{i}{\hbar} \vec{K}_1 \cdot \vec{R}\right) \right| \vec{p}_1+ \right\rangle, \end{aligned} \quad (2)$$

and

$$\mathcal{O} = \left\langle \vec{p}_2- \left| \exp\left(-\frac{i}{\hbar} \vec{K} \cdot \vec{R}\right) \right| \vec{p}_1+ \right\rangle. \quad (3)$$

The symbols \vec{R} and \vec{P} represent, respectively, the position and the momentum operators, $G(\Omega)$ is the Coulomb Green operator, and the two parameters $\Omega_{1,2}$ are given by $\Omega_{1,2} = T_1 - k_{1,2}$.

We have calculated the matrix elements Π_{ij} and \mathcal{O} using integral representations for the Coulomb Green function and the continuum states in the momentum space. The tensor with the components Π_{ij} can be expressed as a linear combination of Kronecker tensor and of tensorial products between the involved momenta:

$$\begin{aligned} \Pi_{ij}(\vec{K}_1, \vec{K}_2, \Omega) &= A \delta_{ij} + B_1^{(0)} p_{1i} p_{1j} + B_1^{(1)} (p_{1i} K_{1j} + p_{1j} K_{1i}) + B_1^{(2)} K_{1i} K_{1j} + B_2^{(0)} p_{2i} p_{2j} + B_2^{(1)} (p_{2i} K_{2j} + p_{2j} K_{2i}) \\ &\quad + B_2^{(2)} K_{2i} K_{2j} + C_1^{(0)} p_{1i} p_{2j} + C_1^{(1,1)} p_{1i} K_{2j} + C_1^{(1,2)} p_{2j} K_{1i} + C_1^{(2)} K_{1i} K_{2j} + C_2^{(0)} p_{2i} p_{1j} \\ &\quad + C_2^{(1,1)} p_{1j} K_{2i} + C_2^{(1,2)} p_{2i} K_{1j} + C_2^{(2)} K_{2i} K_{1j}. \end{aligned} \quad (4)$$

The 15 coefficients of this linear combination are rotationally invariant amplitudes (scalar functions).

Because of orthogonality conditions ($\vec{s}_1 \cdot \vec{K}_1 = \vec{s}_2 \cdot \vec{K}_2 = 0$), the terms containing $B_1^{(2)}$, $B_2^{(2)}$, $C_1^{(1,1)}$, $C_1^{(1,2)}$, and $C_1^{(2)}$ do not contribute to \mathcal{M} . For the remaining ten amplitudes one finds in this way analytic expressions, which are integral

representations involving hypergeometric Gauss functions, very similar in their structure to those used in dipole approximation. Before presenting the amplitudes, we introduce some notations, used in the following:

$$\lambda = \alpha Z m_e c, \quad X^2 = -2m_e \Omega, \quad \eta_{1,2} = \lambda / p_{1,2}, \quad \tau = \lambda / X,$$

$$\alpha_1^\pm = -(p_1 \pm iX)^2 + K_1^2, \quad \alpha_2^\pm = -(p_2 \pm iX)^2 + K_2^2, \quad (5)$$

$$\gamma = -4X^2[(p_1 - p_2)^2 - K^2].$$

We list the expressions for the amplitudes, excepting $C_1^{(0)}$, in the Appendix. The amplitude $C_1^{(0)}$ deserves special attention because it retains a singularity of the matrix element. One can understand this singularity, observing that in the limit $Z \rightarrow 0$ (free electron), the term of zeroth order for

Π_{ij} [Eq. (2)] is proportional with a δ function of momentum transfer $\vec{\Delta}$. Its contribution vanishes because energy conservation does not allow $\vec{\Delta}$ to vanish. As a consequence, the expression for $C_1^{(0)}$ is only apparently of zeroth order in αZ . By an integration by parts, we were able to remove a term, which in fact vanishes and to get an expression for $C_1^{(0)}$ showing its true order in αZ (first order). The expression we get this way is

$$C_1^{(0)} = -\tau(1-i\eta_1)(1-i\eta_2) \frac{K_g}{p_1 p_2} \int_0^1 d\rho \rho^{-\tau} t_a^{1-i(\eta_1+\eta_2)} (-t_{12})^{-2+i\eta_1} t_{21}^{-2+i\eta_2} \\ \times [t_a(1-\rho^2)_2 F_1(2-i\eta_1, 2-i\eta_2; 2; z) + 8\tau X^4 \rho^2 F_1(2-i\eta_1, 2-i\eta_2; 3; z)], \quad (6)$$

where we have defined several functions of the parameters introduced before, and of integration variable, denoted ρ :

$$t_a = (\alpha_1^+ - \alpha_1^- \rho)(\alpha_2^+ - \alpha_2^- \rho) + \gamma \rho, \\ t_{12} = [(\vec{p}_1 - \vec{K}_1)^2 + X^2](1-\rho)(\alpha_2^+ - \alpha_2^- \rho) \\ + 4X^2[(\vec{p}_1 - \vec{K})^2 - p_2^2] \rho, \\ t_{21} = [(\vec{p}_2 + \vec{K}_2)^2 + X^2](1-\rho)(\alpha_1^+ - \alpha_1^- \rho) \\ - 4X^2[p_1^2 - (\vec{p}_2 + \vec{K})^2] \rho,$$

and

$$t_b = [(\vec{p}_1 - \vec{K}_1)^2 + X^2][(\vec{p}_2 + \vec{K}_2)^2 + X^2](1-\rho)^2 + 4X^2 \Delta^2 \rho.$$

The variable z of the hypergeometric Gauss function is $z = 1 - t_a t_b / t_{12} t_{21}$, and the constant K_g has the expression

$$K_g = \frac{8m_e}{\pi^2} \sqrt{p_1^3 p_2^3} X^3 \Gamma(1-i\eta_1) \Gamma(1-i\eta_2) \exp\left(\pi \frac{\eta_2 - \eta_1}{2}\right).$$

We notice that the amplitude $C_1^{(0)}$ is (up to factor) the one Korol [18] denotes by C . Our result is much simpler than his result (36c) in Ref. [18].

We have considered also several limiting cases.

(i) For $\vec{K}_1 = \vec{K}_2 = \vec{0}$ we reobtain the equations of CNRD calculation [8]. Comparing the two sets of equations, one observes that the retardation manifests in two ways: (1) through supplementary terms in Π_{ij} ; and (2) through some modifications of the amplitudes (the variable of Gauss functions and the functions which multiply these ones under integrals are modified and more complicated than in the CNRD calculation).

(ii) For $\alpha Z \rightarrow 0$, keeping only the terms of first order in this parameter (i.e., the contribution of the amplitudes $B_1^{(0)}$, $B_1^{(1)}$, $B_2^{(0)}$, $B_2^{(1)}$, $C_1^{(0)}$, and \mathcal{O}), and neglecting the others (which are of second order), we reobtain the equations of BNRR calculation [16] (note also that in this limit $B_1^{(1)} = -B_1^{(0)}$, and $B_2^{(1)} = B_2^{(0)}$).

(iii) For one low-energy photon (“soft” photon, $k_1 \rightarrow 0$), one obtains an equation in agreement with the general prediction of QED:

$$\mathcal{M} \sim \mathcal{M}^{(s\text{-ph};1)} \equiv -\frac{1}{k_1} (\vec{s}_1^* \cdot \vec{\delta}_1) (\vec{s}_2^* \cdot \vec{T}), \quad (7)$$

where

$$\vec{\delta}_1 = \frac{\vec{p}_1}{1 - (1/m_e c)(\vec{n}_1 \cdot \vec{p}_1)} - \frac{\vec{p}_2}{1 - (1/m_e c)(\vec{n}_1 \cdot \vec{p}_2)}, \quad (8)$$

and

$$\vec{T} = \left\langle \vec{p}_2 - \left| \exp\left(-\frac{i}{\hbar} \vec{K}_2 \cdot \vec{R}\right) \vec{p} \right| \vec{p}_1 + \right\rangle. \quad (9)$$

From the vector \vec{T} is constructed the matrix element of the single bremsstrahlung.

(iv) When both photons have low energy ($k_{1,2} \rightarrow 0$), by keeping in Eq. (1) only the terms corresponding to the amplitudes $B_1^{(0)}$, $B_2^{(0)}$, and $C_1^{(0)}$, and neglecting the others (their contribution is negligible), we obtain an equation which factorizes the contributions of the two photons:

$$\mathcal{M} \sim \mathcal{M}^{(s\text{-ph};2)} \equiv -\frac{\eta_1}{8\pi^2 m_e} \frac{\Gamma(1-i\eta_1)}{\Gamma(1+i\eta_1)} \\ \times \left(\sin \frac{\theta_e}{2}\right)^{2(-1+i\eta_1)} \frac{1}{k_1 k_2} (\vec{s}_1^* \cdot \vec{\delta}_1) (\vec{s}_2^* \cdot \vec{\delta}_2), \quad (10)$$

where $\vec{\delta}_1$ was defined in Eq. (8) and $\vec{\delta}_2$ is obtained from it by changing \vec{n}_1 to \vec{n}_2 . We mention that the Eq. (10) can be obtained from Eq. (7), taking $k_2 \rightarrow 0$, after $k_1 \rightarrow 0$. Equation (10) is valid for nonforward electron scattering ($\theta_e \neq 0$). Equations (7)–(10) show that the retardation effect is present even in the case of soft photons. The retardation effects are present in the denominators of the terms in $\vec{\delta}_1$ and $\vec{\delta}_2$ through the quantities $(\vec{n}_{1,2} \cdot \vec{p}_1)/m_e c$ and $(\vec{n}_{1,2} \cdot \vec{p}_2)/m_e c$, which do not contain the photon magnitudes but only their directions. This result is the same as Eq. (65) of [18]. It is

interesting that a relativistic Born approximation, soft-photon calculation leads to the same result [15], showing that, at least in the two-soft-photon limit there are no relativistic corrections comparable with the corrections shown here. This is in fact the result predicted from QED, by successive application of the low-energy theorem [19].

The existence of the simple relation,

$$\mathcal{M}^{(s\text{-ph};2)} = \frac{\Gamma(1-i\eta_1)}{\Gamma(1+i\eta_1)} \left(\frac{\theta_e}{2} \right)^{2i\eta_1} \mathcal{M}^{(B;s\text{-ph};2)}, \quad (11)$$

between $\mathcal{M}^{(s\text{-ph};2)}$ and its limit $\mathcal{M}^{(B;s\text{-ph};2)}$ in Born approximation is connected with the particularity of the Coulomb field for which, in the nonrelativistic case, the first Born approximation leads to the exact elastic cross section (Rutherford cross section). The difference between the two amplitudes in the preceding relation is a phase factor, irrelevant for the cross sections. This implies that for soft photons the CNRR and BNRR calculations give the same results, even if the conditions for Born approximation to be valid are not fulfilled.

For the case of near forward scattering ($\theta_e \approx 0$), the situation is quite different: in Born approximation one can demonstrate analytically that the terms linear in photon and electron momenta have a contribution of the same order as that of the terms quadratic in electron momenta. We mention that in a CNRR treatment, this property seems to be confirmed by our numerical calculations. As a consequence, for near forward scattering the matrix elements $\mathcal{M}^{(s\text{-ph};2)}$ and $\mathcal{M}^{(B;s\text{-ph};2)}$ differ not only by a phase factor, and also the corresponding cross sections are different.

III. NUMERICAL RESULTS AND CONCLUSIONS

We consider two types of the possible multiple differential cross sections for double bremsstrahlung, denoted by σ_5 and σ_4 . The most completely differential cross section (without observation of electron spin and without photon polarization detection) is obtained from the amplitude \mathcal{M} in Eq. (1) as

$$\sigma_5 = \frac{r_0^2}{2} \frac{k_1 k_2}{m_e c^2 T_1} \sum_{s_1, s_2} |\mathcal{M}|^2. \quad (12)$$

For the experiments performed up to now, the scattered electron being not observed, the quantity of interest is

$$\sigma_4 = \int \sigma_5 d\Omega_e. \quad (13)$$

All the results presented here consider the rather low electron energy of several keV.

We start by illustrating in Fig. 1 the present status of the comparison between theory and experiment for incident electron energies around 10 keV. For this energy range, we refer to Hippler's experimental results, presented in Ref. [3] (to our knowledge, there are no other experimental data). We already have compared a part of Hippler's data with the theoretical results in dipole approximation in a previous paper (Fig. 1 in [11], corresponding to Fig. 1 of [3]). Now we consider the data presented in Fig. 2 of [3]. The comparison

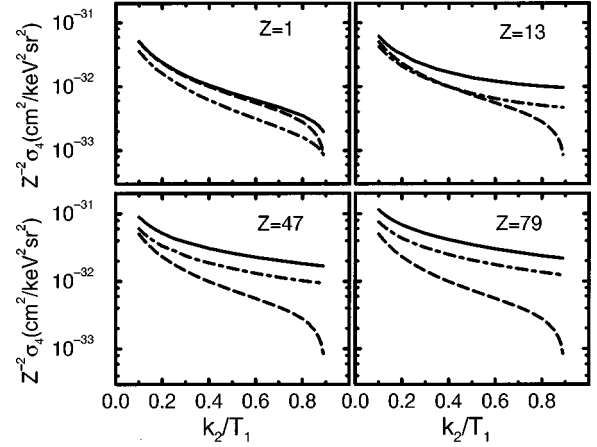


FIG. 2. The values of σ_4/Z^2 in the CNRR (full line), CNRD (dot-dashed line), and BNRR (dashed line) calculations, as a function of the ratio k_2/T_1 , for $T_1=10$ keV, $k_1=1$ keV, and the geometry $\pm 45^\circ$.

is done for the cross section σ_4 , as a function of photon energy k_2 , at $Z=54$, for several values of electron energy T_1 (8.82, 10, and 12.5 keV) and the other photon energy k_1 fixed (2 or 2.8 keV). While for high photon energy k_2 the agreement between theory and experiment is reasonable, one notices a serious discrepancy at low photon energy, not understood up to now.

We mention that all the experimental data of Hippler correspond to a $\pm 90^\circ$ geometry, for which the inclusion of retardation is practically without effect (see also Fig. 3, here). This situation was noticed before, and it is connected with the argument given in Ref. [16], that due to the symmetry of the process amplitudes to the interchange of $\vec{\kappa}_1$ and $\vec{\kappa}_2$, the linear terms in photon momenta in σ_4 will appear only in the scalar product $\vec{p}_1 \cdot (\vec{\kappa}_1 + \vec{\kappa}_2)$, or in the $\pm 90^\circ$ geometry $\vec{p}_1 \cdot \vec{\kappa}_1 = \vec{p}_1 \cdot \vec{\kappa}_2 = 0$. It was one of the conclusions of our previous paper [16] that retardation effects may be suppressed by picking configurations for which $\vec{p}_1 \cdot (\vec{\kappa}_1 + \vec{\kappa}_2) = 0$.

In what follows we shall present theoretical results which

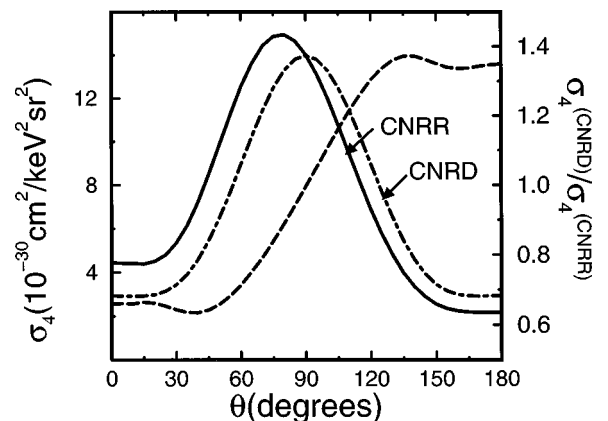


FIG. 3. The cross section σ_4 (CNRR full line, CNRD dot-dashed line), and the ratio $\sigma_4^{(\text{CNRD})}/\sigma_4^{(\text{CNRR})}$ as functions of the angle θ between each photon and the incident electron momentum, for $Z=18$, $T_1=8.82$ keV, $k_1=2.8$ keV, and $k_2=1$ keV.

illustrate the importance of retardation effects for the cross sections σ_4 and σ_5 .

Figure 2 illustrates the Z dependence of retardation effects for σ_4 , in the case of $\pm 45^\circ$ geometry. The four panels, each one corresponding to a different atomic number Z , present a comparison between CNRR (full line), CNRD (dot-dashed line), and BNRR (dashed line) results, for an incident electron energy of 10 keV. The quantity represented is σ_4/Z^2 , as a function of the ratio k_2/T_1 , the energy k_1 of the other photon being fixed at $k_1=1$ keV. One observes that: (1) the dipole approximation is not valid for this energy (a similar conclusion was obtained in Ref. [16], working in Born approximation); (2) the Born approximation is acceptable for the case of the panel corresponding to $Z=1$ (except the case of low final electron energy), but unacceptable for the other cases. Born approximation requires both η_1 and η_2 [Eq. (5)] to be much smaller than 1. At fixed k_1 , η_2 increases with increasing k_2 , up to ∞ , reached for $T_2=0$. This explains why, even for low Z , for k_2 approaching the maximum value T_1-k_1 , Born approximation results deviate from the exact Coulomb ones.

The dipole approximation predicts identical results for the geometries $\pm\theta$ and $\pm(\pi-\theta)$. This symmetry is lost in CNRR theory, as one can see in Fig. 3 (CNRR full line, CNRD dot-dashed line), where we represent the dependence of the cross section σ_4 on the angle θ between each photon momentum and the incident electron momentum. We have considered the process of emission of two photons with energies 2.8 keV and 1 keV, by an electron with the energy 8.82 keV, scattered by a target with $Z=18$ (one of the cases investigated by Hippler [3], but only for the geometry $\pm 90^\circ$). In the CNRR calculation, the emission of photons in the forward directions is more probable than in backward directions. We represent also (dashed line) the ratio of CNRD and CNRR values for σ_4 . This ratio is close to 1 for $\theta=90^\circ$, a feature met also in the Born approximation (see Ref. [16]), and having the explanation mentioned before.

Information about the importance of retardation effects for the most detailed cross section in its dependence on the electron scattering angle θ_e is given in Fig. 4. The left panels, (a) and (c), give CNRR results, and the right panels, (b) and (d), CNRD results. The emission geometries are $\pm 45^\circ$ for upper panels (a) and (b), and $\pm 90^\circ$ for lower panels (c) and (d). The different curves correspond to different values of the electron azimuthal angle ϕ_e , in a reference frame with z axis along the incident electron momentum and the photons in the x - z plane. The energies are $T_1=10$ keV, $k_1=1$ keV, and $k_2=5$ keV. A large retardation effect, strongly dependent on the final direction of the electron, is observed for geometries $\pm 45^\circ$. On the contrary, for geometries $\pm 90^\circ$, the CNRR and CNRD theories give close results.

Finally, in Fig. 5, we consider the emission of two very low-energy photons, namely, $k_1/T_1=k_2/T_1=0.001$, at very low electron scattering angles ($\theta_e < 1^\circ$). Two sets of curves are represented, given by CNRR and BNRR theories. One observes that for $\theta_e > 0.5^\circ$, the two curves practically coincide; this is so, not because the Born approximation is valid, but because for this angular range the matrix elements differ, with a good approximation, only by a phase factor, as explained at the end of Sec. II. The situation is different for

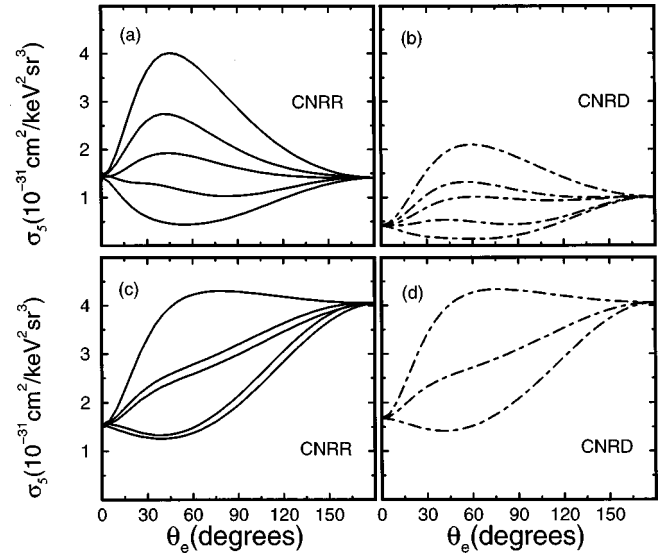


FIG. 4. The cross section σ_5 , as a function of the scattered electron angle θ_e , for $Z=13$, $T_1=10$ keV, $k_1=1$ keV, and $k_2=5$ keV. The upper panels (a) and (b) are for the geometry $\pm 45^\circ$, the lower for $\pm 90^\circ$. In each panel, the curves correspond to different values of the azimuthal angle ϕ_e , starting from below: 180° , 0° , 135° , 45° , and 90° . In (d), the curves for 180° and 0° are identical, as also are those for 135° and 45° .

very small scattering angles $\theta_e < 0.2^\circ$, where Coulomb field effects come into play in a more complicated manner. With all this difference, our numerical results seem to indicate that the order of magnitude of the amplitude \mathcal{M} as function of k_1 and k_2 , in the soft-photon regime, does not change dramatically when approaching the limit of forward scattering. This is in contrast with the results established in [18], for higher electron energies.

In conclusion, our paper demonstrates the importance of the retardation effects in the energy range considered (around 10 keV), for the two-photon bremsstrahlung in the Coulomb field. With the exception of some geometries, these effects cannot be ignored in an exact calculation. Unfortunately,

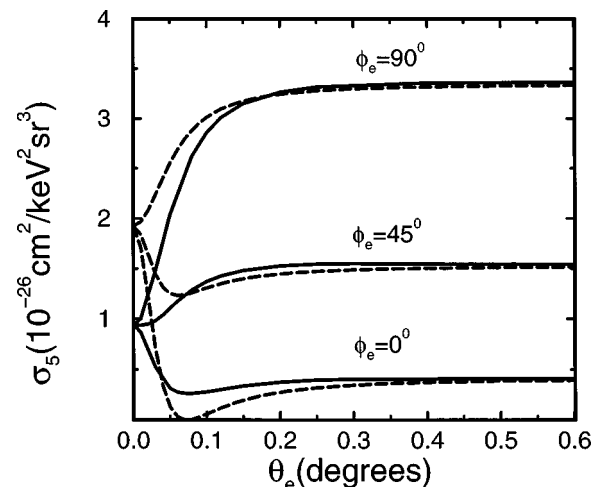


FIG. 5. The values of the cross section σ_5 , in the CNRR (full line) and BNRR (dashed line) calculations as a function of the angle θ_e , for three values ϕ_e ($0^\circ, 45^\circ, 90^\circ$), $Z=13$, $T_1=10$ keV, $k_1=k_2=10$ eV. The emission geometry is $\pm 45^\circ$.

their neglect does not appear to be the cause of the discrepancy between theory and the experimental data of Hippler [3]. For a precise comparison with experimental data screening effects should be included. An opinion on their effect was expressed at the end of Sec. I of Ref. [16]; taking the one-photon bremsstrahlung case as a guide, one may think that they will reduce the value of the cross section, but will still indicate their order of magnitude.

ACKNOWLEDGMENTS

The authors express their gratitude to R.H. Pratt for many discussions on various aspects of two-photon bremsstrah-

lung. The present investigation is directly connected with the cooperative work of one of the authors (V.F.) and R.H. Pratt under a National Research Council Romanian Twinning Program. The work was supported by the Romanian Academy through Grant No. 2928/1997.

APPENDIX: THE EXPRESSIONS OF THE AMPLITUDES

We give here the list of amplitudes which enter in Eq. (4). Some of the notations and the amplitude $C_1^{(0)}$ are given in Sec. II.

$$A = 2 \eta_1 \eta_2 K_g \int_0^1 d\rho \rho^{1-\tau} t_a^{-i(\eta_1+\eta_2)} (-t_{12})^{-1+i\eta_1} t_{21}^{-1+i\eta_2} {}_2F_1(1-i\eta_1, 1-i\eta_2; 2; z), \quad (\text{A1})$$

$$B_1^{(0)} = \gamma_B \int_0^1 d\rho \rho^{1-\tau} t_a^{2-i(\eta_1+\eta_2)} (-t_{12})^{-3+i\eta_1} t_{21}^{-1+i\eta_2} \left[\frac{a_2}{t_a} {}_2F_1(2-i\eta_1, 1-i\eta_2; 2; z) + \frac{1-i\eta_2}{2} \left(\frac{b_2}{t_{21}} - \frac{a_2}{t_a} w \right) {}_2F_1(3-i\eta_1, 2-i\eta_2; 3; z) \right], \quad (\text{A2})$$

with $\gamma_B = 4(1-i\eta_1)(2-i\eta_1)\eta_2(X/p_1)K_g$, $a_2 = \alpha_2^+ - \alpha_2^- \rho^2$, $b_2 = [(\vec{p}_2 + \vec{K}_2)^2 + X^2](1-\rho^2)$, and $w = 1-z$;

$$B_1^{(1)} = -\frac{\gamma_B}{2-i\eta_1} \int_0^1 d\rho \rho^{1-\tau} t_a^{1-i(\eta_1+\eta_2)} (-t_{12})^{-2+i\eta_1} t_{21}^{-1+i\eta_2} [\chi^{(I)} {}_2F_1(2-i\eta_1, 1-i\eta_2; 2; z) + \chi^{(II)} {}_2F_1(3-i\eta_1, 2-i\eta_2; 3; z)], \quad (\text{A3})$$

with

$$\chi^{(I)} = \left(\frac{1-i\eta_1-i\eta_2}{t_a} - \frac{2-i\eta_1}{t_{12}} \right) a_2 - (1-i\eta_2) \frac{b_2}{t_{21}},$$

and

$$\chi^{(II)} = -\frac{(2-i\eta_1)(1-i\eta_2)}{2} \left[\left(\frac{1}{t_a} - \frac{1}{t_{12}} \right) a_2 - \left(\frac{1}{t_{21}} - \frac{1}{t_b} \right) b_2 \right] w,$$

$$C_2^{(0)} = \gamma_{C_2} \int_0^1 d\rho \rho^{2-\tau} t_a^{1-i(\eta_1+\eta_2)} (-t_{12})^{-2+i\eta_1} t_{21}^{-2+i\eta_2} {}_2F_1(2-i\eta_1, 2-i\eta_2; 3; z), \quad (\text{A4})$$

with $\gamma_{C_2} = -8\eta_1\eta_2(1-i\eta_1)(1-i\eta_2)X^2K_g$;

$$C_2^{(1,1)} = -\frac{2\gamma_{C_2}}{1-i\eta_2} \int_0^1 d\rho \rho^{2-\tau} t_a^{-i(\eta_1+\eta_2)} (-t_{12})^{-1+i\eta_1} t_{21}^{-1+i\eta_2} \left[\frac{1}{t_{12}} {}_2F_1(1-i\eta_1, 1-i\eta_2; 2; z) - \frac{1-i\eta_2}{2} \left(\frac{1}{t_{12}} - \frac{1}{t_b} \right) w {}_2F_1(2-i\eta_1, 2-i\eta_2; 3; z) \right], \quad (\text{A5})$$

$$C_2^{(2)} = -16\eta_1\eta_2X^2K_g \int_0^1 d\rho \rho^{2-\tau} t_a^{-i(\eta_1+\eta_2)} (-t_{12})^{-1+i\eta_1} t_{21}^{-1+i\eta_2} [y^{(I)} {}_2F_1(1-i\eta_1, 1-i\eta_2; 2; z) + y^{(II)} {}_2F_1(2-i\eta_1, 2-i\eta_2; 3; z)], \quad (\text{A6})$$

with

$$y^{(I)} = \frac{i(\eta_1 + \eta_2)}{t_a} + \frac{1 - i\eta_1}{t_{12}} + \frac{1 - i\eta_2}{t_{21}},$$

and

$$y^{(II)} = \frac{(1 - i\eta_1)(1 - i\eta_2)}{2} \left(\frac{1}{t_a} + \frac{1}{t_b} - \frac{1}{t_{12}} - \frac{1}{t_{21}} \right) w.$$

The expressions of amplitudes $B_2^{(0)}$, $B_2^{(1)}$, and $C_2^{(1,2)}$ (not listed here) are obtained from the expressions of $B_1^{(0)}$, $-B_1^{(1)}$, and $-C_2^{(1,1)}$ with the interchanges $\vec{p}_1 \leftrightarrow -\vec{p}_2$ and $\vec{K}_1 \leftrightarrow \vec{K}_2$.

For the amplitude \mathcal{O} , using the same technique as for Π_{ij} , and defining new parameters $\tau_a = (p_1 + p_2)^2 - K^2$, $\tau_b =$

$-\Delta^2$, $\tau_{12} = p_2^2 - (\vec{p}_1 - \vec{K})^2$, and $\tau_{21} = p_1^2 - (\vec{p}_2 + \vec{K})^2$, we have established the expression

$$\begin{aligned} \mathcal{O} = & -\frac{K_g}{8} \frac{\lambda}{p_1 p_2 X^3} \tau_a^{-i(\eta_1 + \eta_2)} (-\tau_{12})^{-1+i\eta_1} \tau_{21}^{-1+i\eta_2} \\ & \times \left[(1 - i\eta_1) \left(\frac{p_1 + p_2}{p_1 - p_2} + \frac{\tau_a}{\tau_{12}} \right) {}_2F_1(2 - i\eta_1, 1 - i\eta_2, 2; z_0) \right. \\ & \left. + (1 - i\eta_2) \left(\frac{p_1 + p_2}{p_2 - p_1} + \frac{\tau_a}{\tau_{21}} \right) {}_2F_1(1 - i\eta_1, 2 - i\eta_2, 2; z_0) \right], \end{aligned} \quad (A7)$$

with $z_0 = 1 - \tau_a \tau_b / \tau_{12} \tau_{21}$. One notes that the amplitude \mathcal{O} does not contribute to \mathcal{M} in the dipole approximation (for $K=0$, the coefficients of ${}_2F_1$ functions are zero).

-
- [1] J. C. Altman and C. A. Quarles, Nucl. Instrum. Methods Phys. Res. A **240**, 538 (1985); Phys. Rev. A **31**, 2744 (1985).
 [2] C. A. Quarles and Jingai Liu, Nucl. Instrum. Methods Phys. Res. B **79**, 142 (1993).
 [3] R. Hippler, Phys. Rev. Lett. **66**, 2197 (1991).
 [4] R. Hippler and H. Schneider, Nucl. Instrum. Methods Phys. Res. B **87**, 268 (1994).
 [5] R. H. Pratt, C. D. Shaffer, N. B. Avdonina, X. M. Tang, and V. Florescu, Nucl. Instrum. Methods Phys. Res. B **99**, 156 (1995).
 [6] V. Véniard, M. Gavrila, and A. Maquet, Phys. Rev. A **35**, 448 (1987).
 [7] M. Gavrila, A. Maquet, and V. Véniard, Phys. Rev. A **42**, 236 (1990).
 [8] V. Florescu and V. Djamo, Phys. Lett. A **119**, 73 (1986).
 [9] A. V. Korol, J. Phys. B **27**, 155 (1994).
 [10] A. V. Korol, J. Phys. B **26**, 3137 (1993).
 [11] M. Dondera and V. Florescu, Phys. Rev. A **48**, 4267 (1993).
 [12] A. I. Smirnov, Yad. Fiz. **25**, 1030 (1977) [Sov. J. Nucl. Phys. **25**, 548 (1977)].
 [13] D. L. Kahler, Jingai Liu, and C. A. Quarles, Phys. Rev. Lett. **68**, 1690 (1992).
 [14] Jingai Liu and C. A. Quarles, Phys. Rev. A **47**, R3479 (1993).
 [15] D. Ghilencea, O. Toader, and C. Diaconu, Rom. Rep. Phys. **47**, 185 (1995).
 [16] M. Dondera, V. Florescu, and R. H. Pratt, Phys. Rev. A **53**, 1492 (1996).
 [17] A. V. Korol, J. Phys. B **29**, 3257 (1996).
 [18] A. V. Korol, J. Phys. B **30**, 413 (1997).
 [19] J. M. Jauch and F. Rohrlich, *The Theory of Photons and Electrons* (Springer-Verlag, Berlin, 1976).